Kinectin-mediated endoplasmic reticulum dynamics supports focal adhesion growth in the cellular lamella

Xin Zhang[1,*], Yee Han Tee[2,3,*], Justin K. Heng[2,3], Yajuan Zhu[1,4], Xian Hu[2,3], Felix Margadant[2,3], Christoph Ballestrem[5], Alexander Bershadsky[3,6], Gareth Griffiths[7] and Hanry Yu[1,2,3,8,9,10,11,‡]

[1]Graduate Program in Bioengineering, NUS Graduate School for Integrative Sciences and Engineering, 28 Medical Drive, 117456, Singapore
[2]Department of Physiology, Yong Loo Lin School of Medicine, National University of Singapore, 117597, Singapore
[3]Centre for Mechanobiology, Temasek Laboratories, National University of Singapore, 5A Engineering Drive 1, 117411, Singapore
[4]Department of Immunology, Yale School of Medicine, New Haven, CT 06520, USA
[5]Faculty of Life Sciences, The University of Manchester, Manchester M13 9PT, UK
[6]Department of Molecular Cell Biology, Weizmann Institute of Science, Rehovot, 76100, Israel
[7]IMBV, University of Oslo, 0371, Norway
[8]Institute of Bioengineering and Nanotechnology, A*STAR, 138669, Singapore
[9]Singapore-MIT Alliance, E4-04-10, 4 Engineering Drive 3, 117576, Singapore
[10]Singapore-MIT Alliance for Research and Technology, S16-05-08, 3 Science Drive 2, 117543, Singapore
[11]Department of Mechanical Engineering, Massachusetts Institute of Technology, 77 Massachusetts Avenue, Cambridge, MA 02139, USA
*These authors contributed equally to this work
‡Author for correspondence (phsyuh@nus.edu.sg)

Summary

Focal adhesions (FAs) control cell shape and motility, which are important processes that underlie a wide range of physiological functions. FA dynamics is regulated by cytoskeleton, motor proteins and small GTPases. Kinectin is an integral endoplasmic reticulum (ER) membrane protein that extends the ER along microtubules. Here, we investigated the influence of the ER on FA dynamics within the cellular lamella by disrupting the kinectin–kinesin interaction by overexpressing the minimal kinectin–kinesin interaction domain on kinectin in cells. This perturbation resulted in a morphological change to a rounded cell shape and reduced cell spreading and migration. Immunofluorescence and live-cell imaging demonstrated a kinectin-dependent ER extension into the cellular lamella and ER colocalisation with FAs within the cellular lamella. FRAP experiments showed that ER contact with FAs was accompanied with an increase in FA protein recruitment to FAs. Disruption of the kinectin–kinesin interaction caused a reduction in FA protein recruitment to FAs. This suggests that the ER supports FA growth within the cellular lamella. Microtubule targeting to FAs is known to promote adhesion disassembly; however, ER contact increased FA size even in the presence of microtubules. Our results suggest a scenario whereby kinectin–kinesin interaction facilitates ER transport along microtubules to support FA growth.

Key words: Kinectin, Focal adhesion, Endoplasmic reticulum, Cell spreading, Migration

Introduction

Cellular processes such as cell shape control, spreading and migration have numerous implications in physiological functions such as tissue repair and development, and cancer metastasis (Chambers et al., 2002; Ridley et al., 2003). These cellular processes are driven by membrane extension and focal adhesion (FA) formation at the cell periphery (Lauffenburger and Horwitz, 1996). Membrane extension begins with dynamic changes to the cytoskeleton. These dynamic changes are initiated by polymerisation of actin barbed ends, and this in turn is affected by regulators such as Rho family GTPases and actin-modifying proteins (Cory and Ridley, 2002; Welch and Mullins, 2002). Adherence of membrane extensions to the substratum occurs via integrins and extracellular matrix (ECM) interaction. This induces additional FA protein recruitment and maturation of the adhesions (Ridley et al., 2003). Adhesions serve as traction sites for cell motility and stabilise membrane extensions during cell spreading and migration (Balaban et al., 2001; Zhang et al., 2008). Adhesions are dynamic and diverse, differing in composition, size and behaviour. Adhesions begin as small focal complexes or 'nascent adhesions', which are formed within minutes at peripheral membrane extensions, mainly in the lamellipodia (Alexandrova et al., 2008; Choi et al., 2008; Zaidel-

Bar et al., 2003). Typically, they initially contain integrin β3 and eventually recruit other proteins such as vinculin, paxillin and zyxin, which can link the adhesions to cytoskeleton (Geiger et al., 2009; Humphries et al., 2007; Wolfenson et al., 2009). The recruitment process increases the size of focal complexes from 0.25 μm to FAs of several micrometres (Adams, 2001; Alexandrova et al., 2008).

Increasing evidence suggests that the endoplasmic reticulum (ER) has a role at FAs. Fibronectin-coated beads adherent on the cell surface induce the formation of integrin adhesion complexes (IACs), as well as the recruitment of ER-resident proteins such as kinectin and calreticulin to the IACs (Tran et al., 2002). The ER proteins calnexin and calreticulin are also localised to FAs upon interleukin-1 (IL-1) signalling (Wang et al., 2006); this localisation is a prerequisite for IL-1-induced Ca^{2+} signalling. The ER-bound phosphatase PTP1B, which is essential for adhesion-dependent signalling and cell spreading, has also been shown to localise to newly formed cell–ECM adhesions (Arregui et al., 1998; Hernandez et al., 2006). Although colocalisation of ER proteins with adhesion sites is known, there is a limited understanding of the mechanism by which this occurs.

The ER is a reticulated organelle that spans the entirety of many cell types and is important in protein synthesis, calcium storage

and lipid synthesis (Baumann and Walz, 2001; Taylor et al., 2009). ER morphogenesis is mediated by a combination of mechanisms. Integral ER membrane proteins, the reticulons and DP1/Yop1p, help to curve the ER membrane to generate and maintain the tubular structure of the ER (Hu et al., 2008; Voeltz et al., 2006). Another class of integral ER membrane proteins, CLIMP-63 and kinectin, modulate the ER interaction with the microtubule (MT) cytoskeleton. CLIMP-63 and kinectin act as static and dynamic anchors, respectively, to facilitate ER membrane extension along MTs (Klopfenstein et al., 1998; Santama et al., 2004). Dynamic extension of the ER to FA sites would probably require plus-end-directed transport. Kinesin is the major MT motor protein responsible for plus-end-directed transport of the ER (Wozniak et al., 2009). The kinesin binding partner on the ER is kinectin (Kumar et al., 1995; Toyoshima et al., 1992). Variable domains are present at the kinectin C-terminus (Leung et al., 1996). Among them, variable domains 3 and 4 (vd3 and vd4) have been shown to interact with kinesin (Ong et al., 2000). The minimal kinectin–kinesin interaction domain on kinectin, termed KNT[+], has been identified as amino acid residues 1188–1288, and consists of part of vd3 (residues 1177–1200) and the entire vd4 (residues 1229–1256) (Santama et al., 2004). The minimal kinectin–kinesin interaction domain on kinesin, termed KHC[+], has also been identified and consists of amino acid residues 833–900 (Santama et al., 2004). For cells overexpressing either the KNT[+] or the KHC[+] domain, ER is absent within the cell periphery (Santama et al., 2004). This demonstrates the importance of the kinectin–kinesin interaction in mediating plus-end-directed ER extension to the cell periphery.

In this study, we define the mechanism by which ER is localised to FAs and investigate the influence of ER on FA dynamics. We demonstrate that kinectin–kinesin interaction mediates ER extension into the cellular lamella to colocalise with FAs within the cellular lamella. This kinectin-mediated localisation of the ER

to FAs is essential for FA protein recruitment to FAs. Functional impairment of the kinectin–kinesin interaction reduces the number of FAs formed within the cellular lamella. Aberrant FA dynamics and formation is the probable cause for the morphological change to a rounded cell shape and reduced cell spreading and migration observed in cells with disrupted kinectin–kinesin interaction. Finally, by probing the respective roles of the ER and MTs in regulating FA assembly and disassembly, we show that MTs alone facilitate FA disassembly, whereas ER localisation to FAs promotes their growth, even in the presence of MTs.

Results

Kinectin–kinesin interaction is essential for controlling cell shape, spreading and migration

We have previously established a stable kinectin-knockdown HeLa cell line (Santama et al., 2004). The kinectin knockdown (KNT[KD]) cells exhibited a more rounded morphology than the spread morphology of the vector control (KNT[VC]) and wild-type (KNT[WT]) cells after culture for 12 hours after trypsinisation (Fig. 1A). In long-term cell culture, KNT[KD] cells exhibited rounded colony-like growth, whereas KNT[VC] and KNT[WT] cells appeared more dispersed (Fig. 1B). The colony-like growth of KNT[KD] could be attributed either to stronger cell–cell interactions or reduced cell spreading and motility. A cell spreading assay was performed where trypsinised cells were allowed to reattach and spread overnight. Their projected cell areas were monitored using time-lapse confocal microscopy (Fig. 1C). The initial projected cell area was noted after cell seeding at 0 hour. For KNT[VC] and KNT[WT] cells, projected cell area increased by ~3 times their initial area 12 hours after cell seeding. By contrast, the KNT[KD] projected cell area increased only by ~1.5 times the initial area after 12 hours, demonstrating reduced spreading.

We attempted to rescue KNT[KD] cells by expressing in them either green fluorescence protein (GFP)-tagged cDNA for human
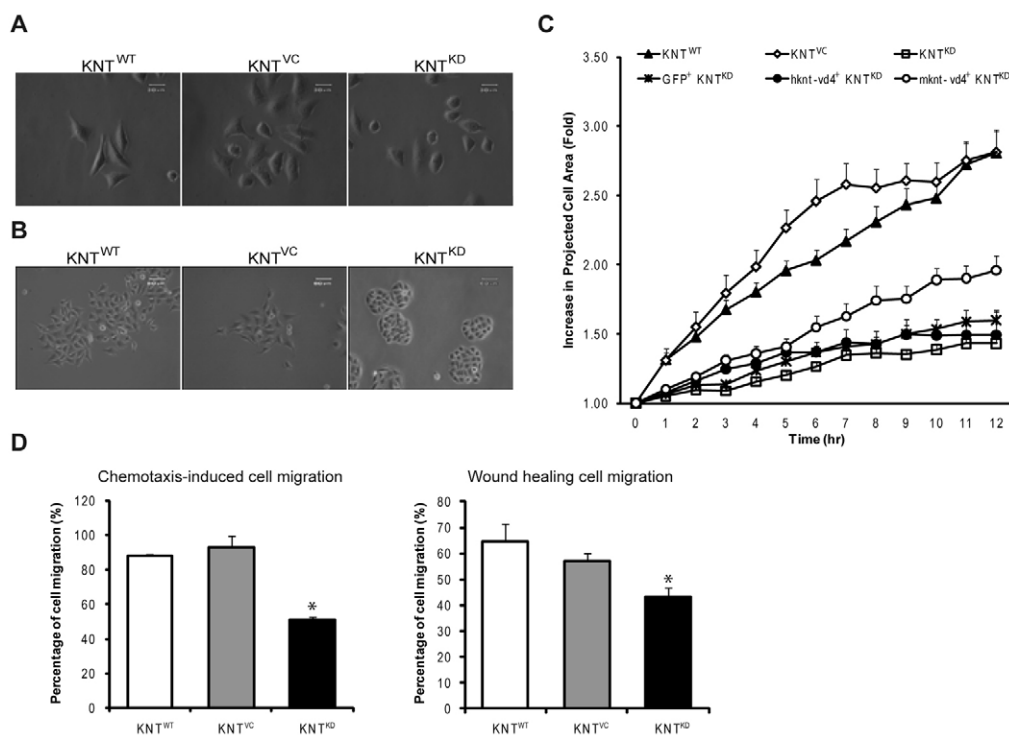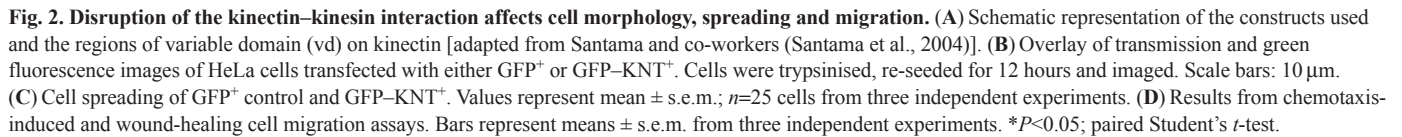

Fig. 1. Kinectin knockdown affects cell morphology, spreading and migration. (A) KNT[WT], KNT[VC] and KNT[KD] HeLa cells imaged with light microscope at 20× magnification. Scale bar: 30 μm. (B) Cell colonies imaged with light microscope at 10× magnification. Scale bars: 60 μm. (C) Spreading of KNT[WT], KNT[VC] and KNT[KD] cells. Values represent mean ± s.e.m. n=25 cells from two independent experiments. In the rescue experiment, spreading of the control GFP[+] KNT[KD] and KNT[KD] cells expressing human (hknt-vd4[+] KNT[KD]) or mouse (mknt-vd4[+] KNT[KD]) kinectin were quantified. Values represent mean + s.e.m. n=25 cells from three independent experiments. (D) Chemotaxis-induced and wound-healing cell migration assays were performed. Bars represent means + s.e.m. from three independent experiments. *P<0.05; one-way ANOVA with Bonferroni post-test.

Fig. 2. Disruption of the kinectin–kinesin interaction affects cell morphology, spreading and migration. (A) Schematic representation of the constructs used and the regions of variable domain (vd) on kinectin [adapted from Santama and co-workers (Santama et al., 2004)]. (B) Overlay of transmission and green fluorescence images of HeLa cells transfected with either GFP+ or GFP–KNT+. Cells were trypsinised, re-seeded for 12 hours and imaged. Scale bars: 10 μm. (C) Cell spreading of GFP+ control and GFP–KNT+. Values represent mean ± s.e.m.; n=25 cells from three independent experiments. (D) Results from chemotaxis-induced and wound-healing cell migration assays. Bars represent means ± s.e.m. from three independent experiments. *P<0.05; paired Student's t-test.

(hknt-vd4+; Fig. 2A) or mouse (mknt-vd4+; Fig. 2A) kinectin. Control cells were KNT^{KD} cells transfected with empty pEGFP vector (GFP+). Cell spreading of GFP-expressing rescued cells and control cells were examined. Rescue was partial using the mouse *Ktn1* clone, whereas the human *KTN1* clone failed to rescue KNT^{KD} (Fig. 1C). KNT^{KD} cells stably express siRNAs against human kinectin. The siRNAs can compete with the rescue human *KTN1* cDNA, making it difficult to achieve the appropriate expression level of the human kinectin protein in KNT^{KD} cells, resulting in the failed rescue. The siRNAs against human kinectin might not compete as efficiently with the mouse *Ktn1* cDNA as with the human *KTN1* cDNA, hence a partial rescue was observed using the mouse *Ktn1* clone. The partial rescue shows that the reduced cell spreading observed in KNT^{KD} cells is due to the loss of endogenous kinectin protein.

We further assessed cell migration activity using both the chemotaxis-induced assay and wound-healing assay. In the chemotaxis-induced assay, cells in serum-free medium migrated past the separating membrane of a Transwell insert towards medium containing 10% serum. The percentage of cell migration refers to the percentage of cells that migrated across the membrane. In the wound-healing assay, a 'wound' was created in a cell monolayer, and cells migrated to close the wound. The percentage of cell migration measures the wound closure after 24 hours. KNT^{KD} cells exhibited a 38.85±2.85% and 41.75±5.87% reduced migration across the membrane in the chemotaxis-induced assay compared with KNT^{WT} and KNT^{VC} cells respectively (Fig. 1D). The wound

closure of KNT^{KD} cells in the wound-healing assay is also reduced by 21.07±4.01% and 13.41±0.53% when compared against the wound closure of KNT^{WT} and KNT^{VC} cells, respectively (Fig. 1D). These results indicate that kinectin is important in the control of cell shape, spreading and migration.

Kinectin interacts with kinesin KIF5 via a minimal binding domain (KNT+; Fig. 2A) to extend the ER into the cell periphery (Santama et al., 2004). We specifically perturbed this interaction by overexpressing a fusion construct of GFP to KNT+ (GFP–KNT+) in HeLa cells. We assessed the changes in cell shape, spreading and migration of the GFP–KNT+-overexpressing cells versus control cells transfected with the empty pEGFP-C1 vector (GFP+). There was a marked difference in morphology of the cells re-seeded for 12 hours after trypsinisation (Fig. 2B). GFP–KNT+ cells appeared rounded whereas the GFP+ control cells were spread out. Quantitatively, GFP–KNT+ cells spread out to ~1.5 times the initial projected cell area compared with GFP+ control cells, which spread to around three times the initial projected cell area (Fig. 2C). Similarly, compared with GFP+ control cells, GFP–KNT+ cells showed 33.39±6.54% and 33.77±0.40% reduced migration in the chemotaxis-induced and wound-healing assays, respectively (Fig. 2D). We corroborated the effect of disrupting the kinectin–kinesin interaction on cell migration, by overexpressing a GFP-tagged kinectin minimal binding domain on kinesin heavy chain (GFP–KHC+; Fig. 2A) in HeLa cells. Similarly to GFP–KNT+ cells, GFP–KHC+ cells showed 37.58±11.41% and 30.24±2.21% reduced migration
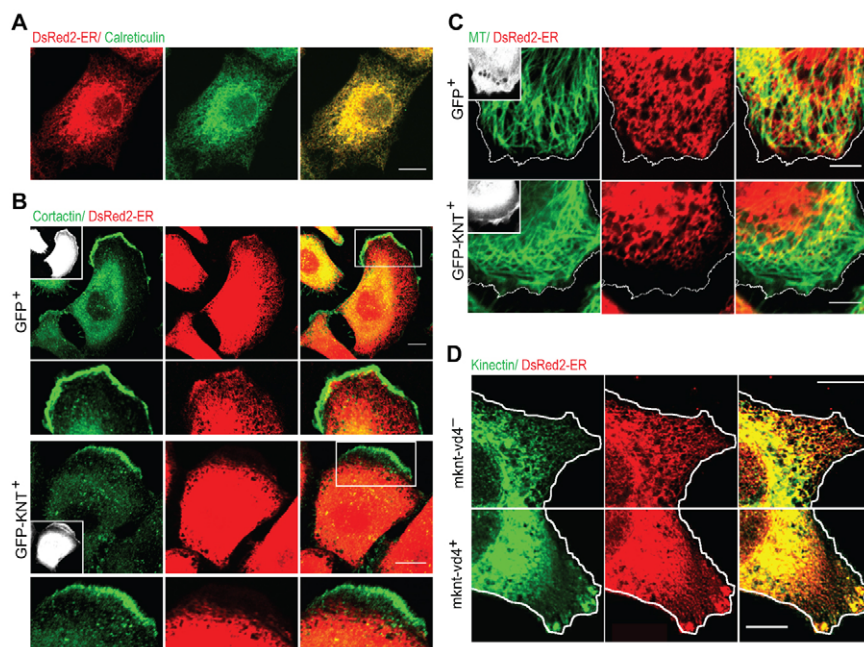
Fig. 3. ER extension into cellular lamella is impaired in GFP–KNT⁺ cell. (A) pDsRed2-ER was stably transfected into HeLa cells to generate a stable DsRed2-ER cell line. ER network (DsRed2-ER) colocalised with calreticulin staining. Scale bars: 10 μm. (B) DsRed2-ER cells were transfected with either GFP⁺ or GFP–KNT⁺ and labelled with anti-cortactin antibodies. ER is absent in the cellular lamella of GFP–KNT⁺ cells. For this and subsequent images, GFP expression is represented as a gray-scale image inset whereas Alexa Fluor 405 secondary antibody labelling is false-coloured green. The centre region of the cell is deliberately saturated for better visualisation of peripheral ER. The lower small panels are enlarged images of the cellular lamella (white box). Scale bars: 10 μm. (C) GFP⁺ or GFP–KNT⁺ transfected DsRed2–ER cells were labelled with anti-tubulin antibody. MT cytoskeleton was unaffected in GFP⁺ and GFP–KNT⁺ cells. Scale bar: 5 μm. (D) Cells were microinjected with either GFP-tagged mouse kinectin containing vd4 (mknt-vd4⁺) or without vd4 (mknt-vd4⁻) constructs and examined for ER and kinectin accumulation at cell periphery. Scale bars: 5 μm.

compared with the GFP⁺ control in chemotaxis-induced and wound-healing assays, respectively (supplementary material Fig. S1A).

To investigate whether the suggested effect of the kinectin–kinesin interaction on cell migration is related to its role in mediating ER transport along MTs, we used siRNA to knock down CLIMP-63 (supplementary material Fig. S2A), which forms a static link between the ER and MTs (Klopfenstein et al., 1998). The control cells (CLIMP-63⁺, siRNA against scrambled sequence) exhibited a normal reticulated distribution of the ER network which extended to the cell edges, whereas CLIMP-63^{KD} cells exhibited faint and diffused ER tubules in the cell periphery, and even these were distant from the cell edges (supplementary material Fig. S2B). In both chemotaxis-induced and wound-healing assays, CLIMP-63^{KD} cells exhibited significantly retarded migration activity (supplementary material Fig. S2C). Therefore, blockade of ER transport along MTs by ER-specific CLIMP-63 disruption had a similar phenotypic effect on cell migration as that observed by disrupting the kinectin–kinesin interaction. These results support the hypothesis that the kinectin–kinesin interaction is important in the control of cell shape, cell spreading and cell migration, possibly by mediating plus-end-directed ER transport along MTs.

Kinectin–kinesin interaction mediates ER extension into cellular lamella

To examine ER dynamics within the cell, we generated a stable cell line that expressed the pDsRed2-ER vector. This vector encodes a fusion red fluorescence protein (DsRed2-ER) – the 5′ end of the red fluorescence protein (DsRed2) is fused to the ER targeting sequence of calreticulin whereas the 3′ end is fused to the ER retention sequence KDEL. Cells stably expressing DsRed2-ER contained red fluorescently labelled ER and were immunolabelled for calreticulin, an ER lumenal protein (Fig. 3A). The DsRed2-ER fluorescence exhibited a high degree of colocalisation with calreticulin, confirming its specificity in labelling the ER. The ER network in DsRed2-ER cells exhibited a well-defined reticulated structure that extended close to the cell edge.

Cellular lamellum is the leading edge of a motile cell, of which the lamellipodium is the most forward portion (Abercrombie et al., 1971; Chhabra and Higgs, 2007; Hinz et al., 1999; Ingram, 1969). To determine the cellular lamella region, we identified the lamellipodia with cortactin. Cortactin is an actin-binding protein that is enriched within and found throughout the lamellipodia (Lai et al., 2008; Weed et al., 2000). We examined ER distribution within the cellular lamella of GFP⁺ control and GFP–KNT⁺ cells. The ER did not colocalise with cortactin in GFP⁺ control or GFP–KNT⁺ cells, indicating the absence of ER within lamellipodia (Fig. 3B). This is consistent with previous report that the lamellipodium is devoid of organelles (Abercrombie et al., 1971). Although the ER network was found within the cellular lamella in GFP⁺ control cells, it was distinctly absent from the cellular lamella of the GFP–KNT⁺ cells (Fig. 3B). This suggests that ER extension into the cellular lamella in GFP–KNT⁺ cell is impaired. For this and subsequent images, GFP expression was represented as a gray-scale image inset whereas Alexa Fluor 405 secondary antibody labelling was false-coloured green. Quantification verified this visual impression; 73.1±21.7% of GFP⁺ control cells compared with a significantly lower 21.1±6.5% of GFP–KNT⁺ cells had ER networks that extended to within 5 μm of the cortactin border at the cellular lamella. Expression of GFP–KNT⁺ or GFP⁺ had no effect on the distribution and morphology of the MT network within the cellular lamella (Fig. 3C). Similarly to overexpression of GFP–KNT⁺ in cells, GFP–KHC⁺ specifically disrupted the kinectin–kinesin interaction without affecting MTs and prevented ER extension on MTs into the cellular lamella (supplementary material Fig. S1B).

We microinjected the GFP-tagged mouse Ktn1 clone containing vd4 (mknt-vd4⁺; Fig. 2A) into DsRed2-ER cells. This resulted in a rapid accumulation of ER and mouse kinectin at the cell periphery in 55.3±2.8% of the microinjected cells after 5 hours. This contrasted significantly with result in cells microinjected with a GFP-tagged mouse Ktn1 clone lacking vd4 (mknt-vd4⁻; Fig. 2A), of which only 3.0±2.2% demonstrated a similar accumulation (Fig. 3D). Taken together with the known kinectin
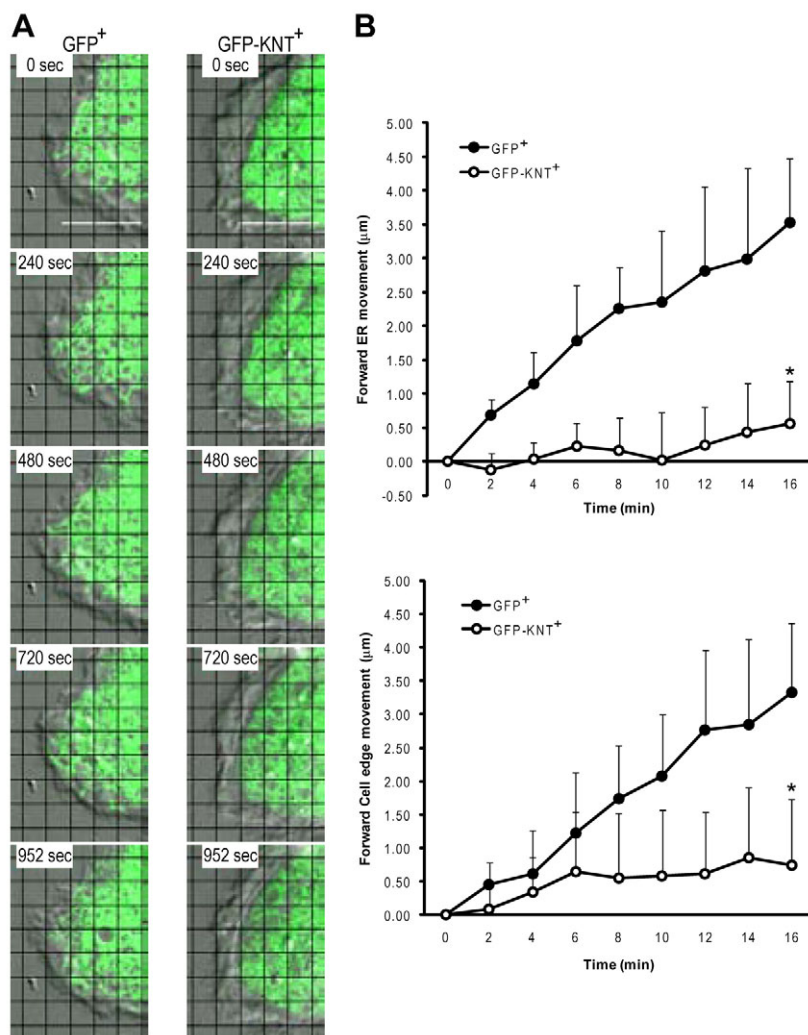
Fig. 4. Kinectin–kinesin interaction mediates ER extension into cellular lamella. (**A**) Selected image sequences from the live imaging of DsRed2-ER cells overexpressing GFP[+] or GFP–KNT[+]. In the overlays, green pseudo-colour indicates ER network. No distinct ER extension into the cellular lamella is observed in GFP–KNT[+] cell compared with control GFP[+] cell. Full-length sequences are provided as supplementary material Movie 1. Scale bars: 10 μm. (**B**) Measurement of the forward ER and cell edge movement. Forward cell membrane extension and ER extension into the cellular lamella is significantly reduced in GFP–KNT[+] cell compared with control GFP[+] cell. Values represent means + s.d.; n=5 cells for each experimental condition. *P<0.05; paired Student's t-test.

function as a dynamic anchor of the ER on MTs, these findings support the hypothesis that the kinectin–kinesin interaction is required for extending the ER along MTs into the cellular lamella to support cell motility such as spreading or migration. Next, we used live-cell confocal microscopy to examine ER extension into the cellular lamella.

Morphologically, the lamella has been described as a flat and sheet-like extension that terminates at the ruffling lamellipodia (Ballestrem et al., 2000; Heath and Holifield, 1991). The region of ruffling lamellipodia at the cell edge of a flat membrane extension represents the cellular lamella. Ruffling lamellipodia can be identified in differential interference contrast (DIC) images of fixed cells as membrane folds at the cell edge or in live cells as retrograde moving undulating membrane at the cell edge. In control cells overexpressing GFP[+], ER tubules (green pseudo-colour) were observed to extend into the cellular lamella and there was forward membrane protrusion (DIC) (Fig. 4A, left panel; see supplementary material Movie 1). However, in cells overexpressing GFP–KNT[+], ER tubules did not extend into the cellular lamella, and the ER remained at a distance from the membrane protrusion. There was also a reduction in forward membrane protrusion in GFP–KNT[+] compared with GFP[+] control cell (Fig. 4A, right panel; see supplementary material Movie 1).

The ER extension into the cellular lamella and forward cell edge movement were measured in GFP–KNT[+] and GFP^{+} control cells (Fig. 4B). The measurements were consistent with the above observations; ER extension into the cellular lamella and forward cell edge movement were significantly reduced in GFP–KNT^{+} cells compared with GFP^{+} control cells. Live-cell confocal microscopy of the ER in GFP–KHC^{+} cells supported the above result from GFP–KNT^{+} cells. The ER in GFP–KHC^{+} cells could not extend into the cellular lamella and there was no observable forward cell edge movement (supplementary material Fig. S1C and Movie 2).

We also noted that GFP–KNT^{+} cells exhibited persistent membrane ruffling at the cell edge without forward movement. Membrane ruffles are initiated within lamellipodia when cell membrane fails to attach to the substratum (Borm et al., 2005). Membrane attachment to the substratum stabilises membrane protrusion; this is an important step preceding forward cell edge movement (Ridley et al., 2003; Zhang et al., 2008). Persistent membrane ruffling at the cell edge without forward movement, as seen in GFP–KNT^{+} cells, suggests that kinectin-mediated ER extension into the cellular lamella has a role in promoting adherence of the cell membrane to the substratum to support further forward cell movement.
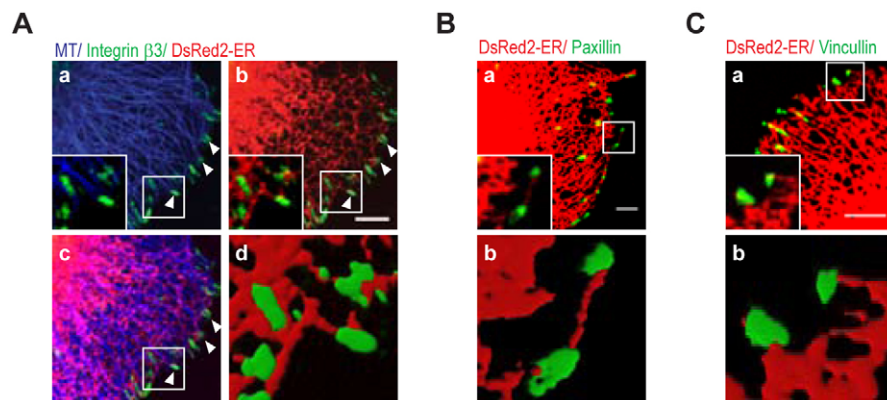
Fig. 5. ER and MT co-localise with integrin β3, paxillin and vinculin FA plaques. (A) DsRed2-ER cells were transfected with GFP-tagged integrin β3 and labelled with anti-tubulin antibodies. Individual ER and MTs were observed to both extend to integrin β3 plaques (white arrowhead). A section of integrin β3 plaque contacted by an ER tubule (white box, d) was surface-rendered. (**B**) Paxillin and (**C**) vinculin were similarly labelled with anti-paxillin and anti-vinculin antibodies respectively in DsRed2-ER cells. Paxillin (Bb) or vinculin (Cb) FA plaques with individual ER tubules extending toward them (white box) were rendered. Images inset are the enlarged images of the respective white boxed-region without surface rendering. Scale bars: 5 μm.

ER tubules extend on MTs to contact FAs and support their growth within the cellular lamella

FA formation is essential for cell membrane attachment to the substratum to stabilise membrane protrusions (Zhang et al., 2008). Kinectin-mediated ER extension into the cellular lamella might be important for FA formation to stabilise the membrane protrusion via adherence to the substratum to bring about further membrane protrusion and forward movement. The ER might contribute to FA dynamics through ER-bound proteins such as PTP1B, which was observed to localise to FAs and mediate adhesion formation (Hernandez et al., 2006). We therefore examined the role of kinectin-mediated ER tubule extension into the cellular lamella on FA proteins within this lamella. We transfected GFP-tagged integrin β3 into DsRed2-ER cells and immunolabelled MTs to examine their relative spatial distributions within the cell. ER tubules run parallel to MTs, leading to integrin-β3-containing FA plaques in the cellular lamella (Fig. 5Aa-c, white arrowheads). Surface rendering of a region of the cell edge (Fig. 5, white boxes) revealed ER tubules that extend to and contact the FA plaques containing integrin β3 (Fig. 5Ad), paxillin (Fig. 5Bb) and vinculin (Fig. 5Cb).

In live-cell confocal microscopy of DsRed2-ER cells expressing GFP-tagged integrin β3 (Fig. 6A; supplementary material Movie 3), ER tubules were observed to extend towards a pre-existing nascent integrin-β3-containing FA plaque (Fig. 6A, white arrowhead), which started growing in size upon ER contact. The ER-contacted FA plaque enlarged to 3.3 times its initial size after 10 minutes, with the ER tubule forming a part of the reticulated ER network after 8 minutes. Therefore, although the formation of nascent FAs is not dependent on the ER (Fig. 6A, 0 minute), FA growth in the cellular lamella is apparently ER dependent.

Fluorescence recovery after photobleaching (FRAP) was performed to determine whether integrin β3 molecules were recruited into FAs to support the ER-dependent FA growth (Fig. 6B). In DsRed2-ER cells expressing GFP-tagged integrin β3, a region containing integrin β3 plaques both with and without ER contact was selected for photobleaching (Fig. 6B, white box). Photobleaching was considered effective because the integrin β3 plaques were not detectable after photobleaching. The ER appeared to gradually recruit integrin β3 to the ER-contacted FA plaques (Fig. 6B, white arrowhead), resulting in recovery of the fluorescence signals within the plaques. The integrin-β3-containing FAs not contacted by ER tubules (white arrow) remained undetectable 20 minutes after photobleaching. FRAP measurement of plaques in contact (ER+) or not (ER–) with ER shows the strongly recovered

fluorescence when the plaque was in contact with the ER, but weakly recovered fluorescence when the ER was not in contact (Fig. 6C). The half-life ($t_{1/2}$) was determined to be ~14.4 minutes for ER+ plaques but indeterminately long for ER– plaques within the experimental time frame. This ER-dependent recruitment of integrin β3 suggests that ER extension to contact FAs is important for FA protein recruitment for FA growth.

Kinectin-mediated ER extension is required for ER-dependent FA protein recruitment in cellular lamella

We further investigated whether it is the kinectin-mediated ER extension into the cellular lamella that supports FA protein recruitment for adhesion growth. We examined established FAs in DsRed2-ER cells overexpressing GFP+ or GFP–KNT+ (Fig. 7A,B). In GFP+ control cells, a normal ER network was observed throughout the cell with distinct paxillin- and vinculin-containing FA plaques distributed within the cellular lamella. When ER networks were retracted in GFP–KNT+ cells, the bulk of the remaining FAs redistributed away from the cellular lamella. The number of FA plaques within 5 μm of the cell edge normalised to the perimeter of the cellular lamella was quantified (Fig. 7C,D). The number of plaques in GFP–KNT+ cells was significantly reduced (peaks at 0.1–0.2 plaques/μm and 0-0.1 plaques/μm, for paxillin and vinculin, respectively) compared with the GFP+ control cells (peaks at 0.2–0.3 plaques/μm for both paxillin and vinculin). The number of vinculin plaques was also visibly reduced within the cellular lamella of GFP–KHC+ cells (supplementary material Fig. S1B). Therefore, kinectin-mediated ER extension on MTs is required for the ER-dependent recruitment of FA proteins to support FA growth within the cellular lamella.

ER- and MT-mediated FA assembly and disassembly

Kinectin-mediated ER extension on MTs supporting FA assembly within the cellular lamella seems contradictory to the established role of MTs in inducing FA disassembly (Bershadsky et al., 1996; Kaverina et al., 1999). We thus compared the roles of the ER and MTs in FA assembly and disassembly by treating DsRed2-ER cells with nocodazole and immunolabelling with either anti-tubulin or anti-vinculin antibodies (Fig. 8). The MT cytoskeleton was observed to be depolymerised after 2 hours of treatment with 1 μM nocodazole (Fig. 8A). Vinculin adhesion plaques were significantly enlarged in nocodazole-treated cells and appeared throughout the cell versus the predominately peripheral distribution of the smaller FAs in the DMSO-treated control cells (Fig. 8A,B). The appearance of adhesions in the central region of the cell might be a result of
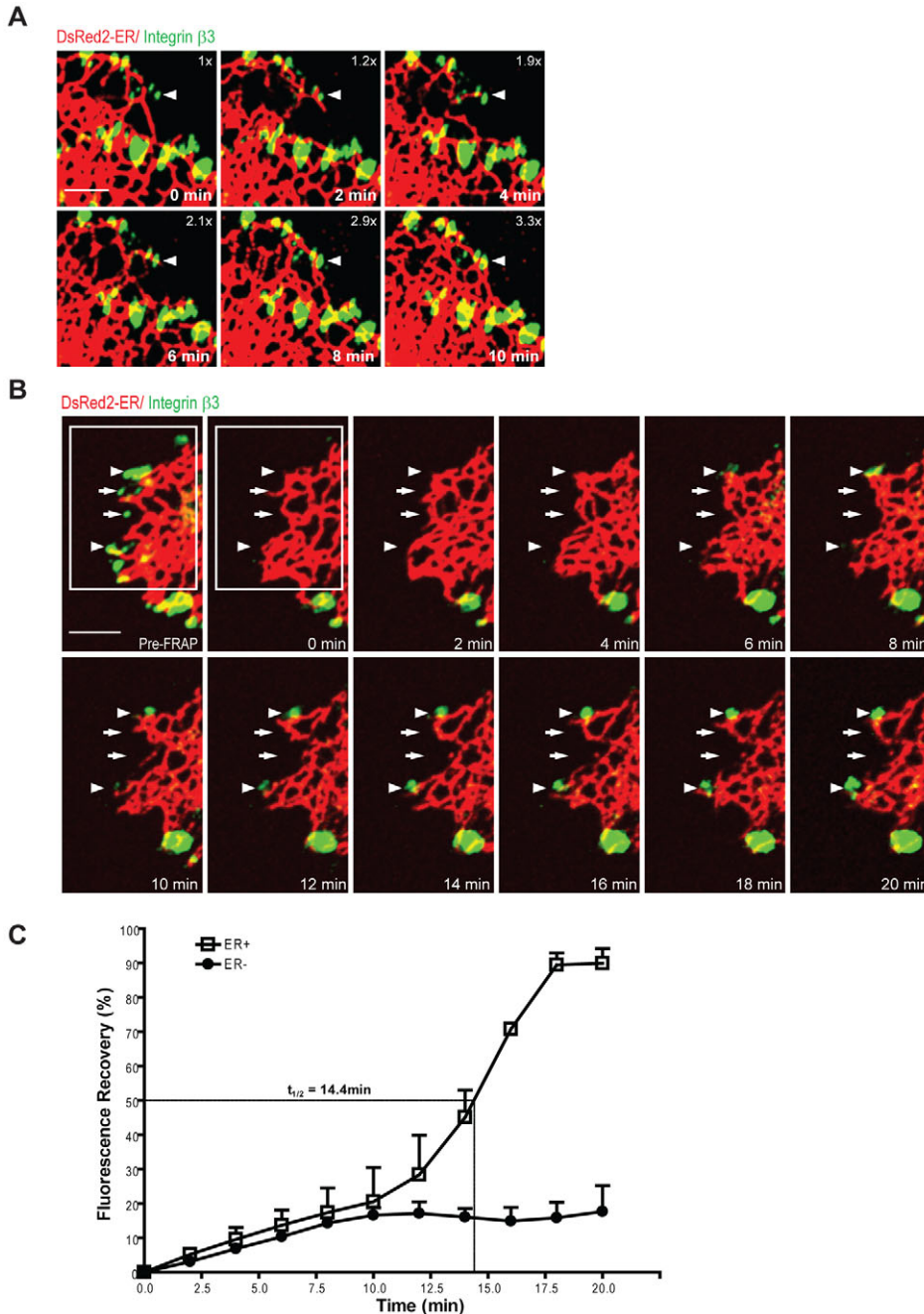
Fig. 6. ER extension to FAs is required for integrin β3 protein recruitment. (**A**) ER tubule extends to contact nascent integrin β3 plaques (live imaging at 20 second intervals, arrowhead). The ER tubule integrates into a characteristic ER network whereas the integrin β3 plaque becomes larger over time. Inset values are the fold increase (×) in plaque size. Full-length sequences are provided as supplementary material Movie 3. (**B**) DsRed2-ER cells were transfected with GFP-tagged integrin β3 and observed under live imaging at 2 minute intervals. A region with numerous integrin β3 plaques was photobleached (box). Recovery of integrin β3 plaque fluorescence was only observed at sites in contact with the ER (arrowhead). Plaques that subsequently did not have contact with ER (arrow) had no notable recovery of fluorescence. Scale bars: 5 μm. (**C**) Graph of fluorescence recovery after bleaching of plaques in contact (ER+) or not in contact (ER−) with ER. Within the experimental time frame, fluorescence is strongly recovered when plaque is in contact with the ER but weakly recovered when ER is not in contact. $t_{1/2}=\sim 14.4$ minutes for ER+ plaques but indeterminately long for ER− plaques. Values represent means + s.e.m.; $n=5$ plaques from two independent experiments for each experimental condition.

slower plaque turnover because of reduced adhesion disassembly in nocodazole-treated cells, leading to the enlargement of plaques previously not observed in the central region of the cell. This is consistent with a MT disruption study where, upon MT network recovery after nocodazole treatment, a greater number of FAs were disassembled in the central region of the cell than the cell periphery (Kaverina et al., 1999).

Although ER extension on MTs was inhibited upon nocodazole treatment, colocalisation of ER markers with vinculin was still visible in the cell periphery (Fig. 8B). Because we have demonstrated that ER contact with FAs can contribute to FA growth at the cell periphery, we correlated ER contact with FA size at the cell periphery in DMSO- and nocodazole-treated cells (Fig. 8B,C). FA size was quantified for vinculin-containing FA plaques in contact with ER (Fig. 8B, white arrowhead) or not in contact with ER (Fig. 8B, white arrow) at the cell periphery. In DMSO-treated control cells, where the MT network was intact (MT+), plaques were larger (0.833 ± 0.054 μm^2) when contacted by ER (ER+) compared with plaques not contacted by ER (ER−; 0.406 ± 0.036 μm^2). In nocodazole-treated cells (MT−), plaques contacted by the ER were similarly observed to be larger (1.717 ± 0.120 μm^2) compared with the non-contacted plaques (0.862 ± 0.081 μm^2) (Fig. 8C). Similar results were obtained with another FA marker, paxillin (supplementary material Fig. S3). Our data suggest that the ER and MTs have antagonistic roles, where the concurrent presence or absence of MTs and ER results in basal level sizes of FA plaques. However, in the absence of either ER or MTs contacts, FA plaque sizes were significantly reduced or increased, respectively. This is
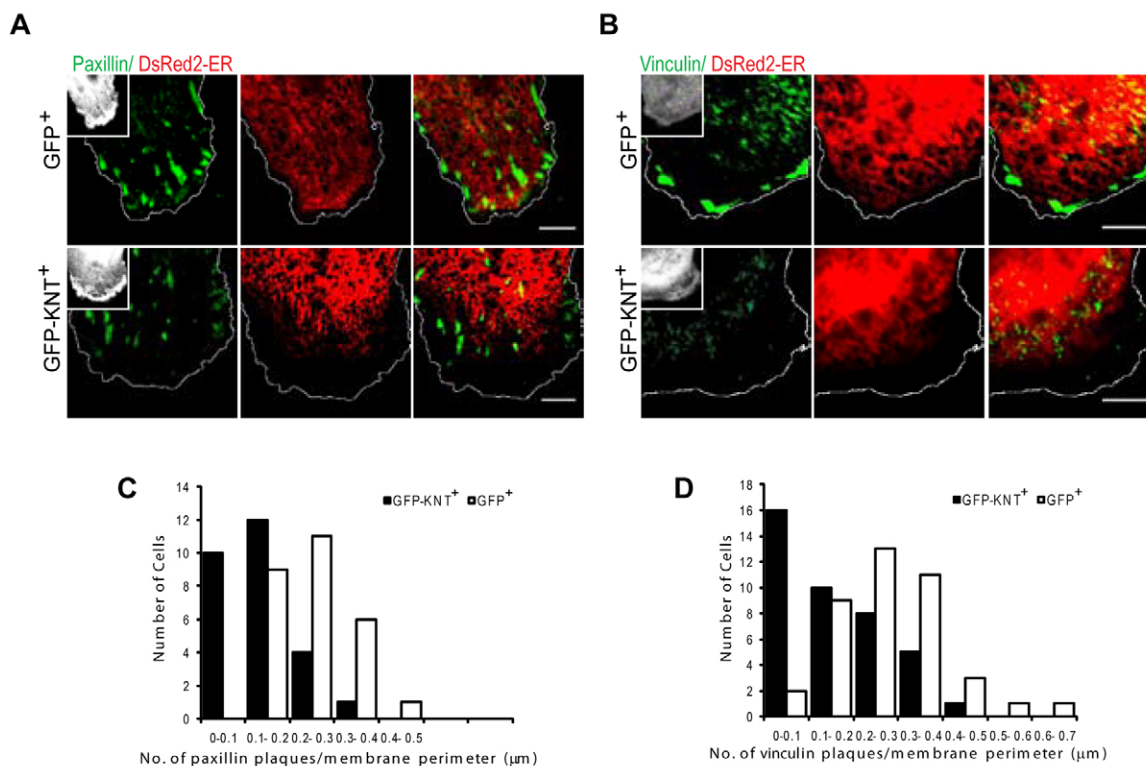
Fig. 7. Disruption of ER extension inhibits FA formation within cellular lamella. DsRed2-ER cells were transfected with GFP[+] or GFP–KNT[+] and immunolabelled with either (**A**) anti-paxillin or (**B**) anti-vinculin antibodies. ER extension to cellular lamella was inhibited in GFP–KNT^{+} cells and cells had reduced plaque formation. GFP^{+} cells in contrast had a well-extended ER network and plaques formed in cellular lamella. Images inset are GFP channel images denoting region of interest in transfected cells. Scale bars: 5 μm. Quantification of the number of (**C**) paxillin (*n*=27 cells per experimental condition) and (**D**) vinculin (*n*=40 cells per experimental condition) plaques within 5 μm of cellular lamella were normalised to the perimeter of their respective membrane ruffles in GFP[+] and GFP–KNT^{+} cells.

consistent with the known role of MTs in facilitating FA disassembly, and our hypothesis that ER contact facilitates FA growth.

Discussion

MT-dependent ER tubule extension and targeting to newly formed focal complexes has been previously demonstrated (Hernandez et al., 2006). Colocalisation of ER-bound PTP1B with various adhesion proteins was abolished by nocodazole treatment, but the exact players involved in this ER–MT–FA colocalisation remain unclear. Here, we provide new insight into the mechanism by which ER localises to FAs and investigate the influence of ER and MTs on FA dynamics.

Kinectin, an integral ER protein, serves as a receptor for interaction with the MT motor kinesin (Kumar et al., 1995; Toyoshima et al., 1992). Kinectin is strongly recruited to the IAC but its functional role at the adhesion site has not been elucidated (Tran et al., 2002). Given its known role in mediating anterograde movement of the ER on MTs (Ong et al., 2000), we investigated the potential role of kinectin in mediating ER extension in the cellular lamella to interact with FAs. Immunofluorescence and live-cell imaging demonstrated a kinectin-dependent ER extension into the cellular lamella and ER colocalisation with FAs within the cellular lamella. This study is possible because of the specific disruption of the ER, but not MTs, in the cellular lamella. In comparison, drugs such as nocodazole cause depolymerisation of the MTs and collapse of the entire cellular ER network, as well as

several pathway failures (Terasaki et al., 1986). Thus, it is noteworthy that only the kinectin–kinesin interaction, not the MT cytoskeleton, was specifically affected in the cellular lamella of the GFP–KNT[+] and GFP–KHC^{+} cells.

In live imaging and FRAP experiments, we observed that ER extension to integrin β3 plaques serves as a prerequisite for integrin β3 protein recruitment and consequent growth of plaques. Signalling by integrins is an important event that initiates recruitment of other adhesion proteins (Berman et al., 2003; Vicente-Manzanares et al., 2009). The recruitment of other adhesion proteins might also occur in an ER-dependant manner, as indicated by the decreasing numbers of vinculin and paxillin plaques in GFP–KNT[+] and GFP–KHC^{+} cells with disrupted kinectin–kinesin interaction. In the absence of adhesion formation in the cellular lamella of GFP–KNT[+] and GFP–KHC^{+} cells, membrane protrusions are not stabilised and fold back on themselves, generating continuous membrane ruffles without the forward movement of cell membrane. By contrast, cell membrane moves forward in GFP^{+} control cells via the formation of new adhesions to stabilise the membrane, before further membrane protrusion. The ER tubules extended at the membrane protrusion might have quelled membrane ruffling by promoting FA development, which facilitates membrane attachment to the substratum. As such, aberrant peripheral membrane protrusion and adhesion formation are the likely causes for the observed reduction in spreading and migration of KNT[KD], GFP–KNT[+] and GFP–KHC^{+} cells. Furthermore, the results that ER networks disrupted by siRNA
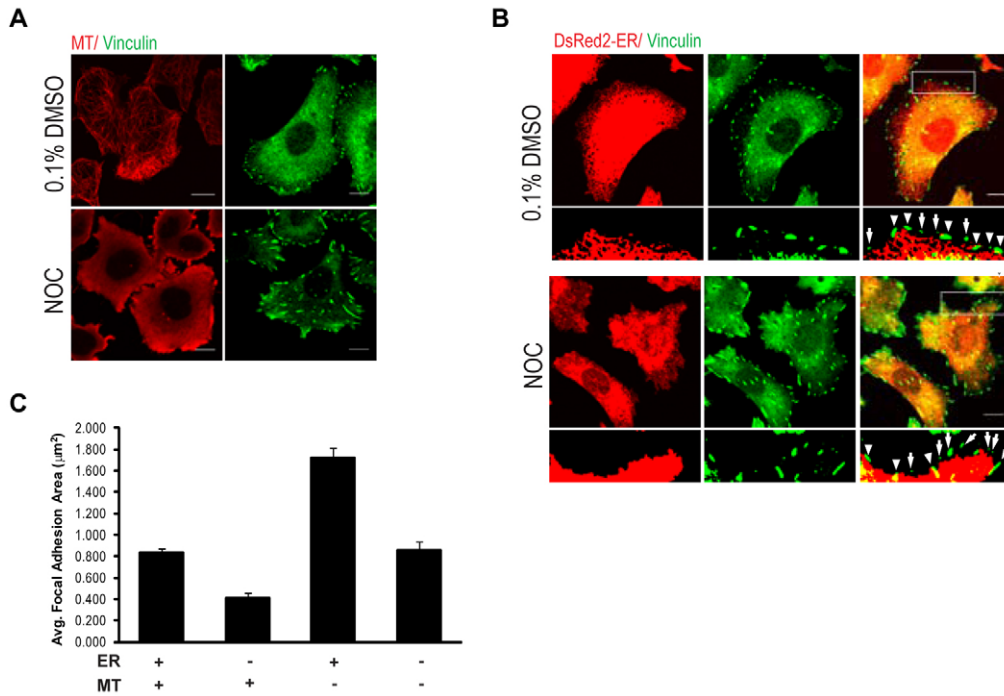
Fig. 8. Roles of ER and MTs in modulating adhesion assembly and disassembly. (**A**) MT-mediated FA disassembly. DsRed2-ER cells were treated with 1 µM nocodazole (NOC) for 2 hours and immunolabelled with either anti-tubulin or anti-vinculin antibodies. Control cells were treated with 0.1% DMSO. MT cytoskeleton was disrupted after nocodazole treatment and vinculin-containing plaques were larger than in DMSO control cells. (**B**) Correlation between ER contact and vinculin FA plaque size in DMSO control and nocodazole-treated cells. The lower small panels are the image-segmented regions (white box in the panel) to identify the FA plaques in contact (white arrowhead) or not in contact with ER (white arrow) at cell periphery. (**C**) Quantification of FA plaque size in contact with ER (ER+) or not in contact with ER (ER–) at the cell periphery in 0.1% DMSO-treated cell (MT+) or nocodazole-treated (MT–) cell. Bars represent means ± s.e.m. *n*=200–500 plaques from 20 cells for each experimental condition. Scale bars: 10 µm.

knockdown of CLIMP-63 could inhibit cell migration corroborate our conclusions derived from KNT+ and KHC+ overexpression experiments on the role of ER in mediating cell migration.

MT depolymerisation by nocodazole leads to enlarged FAs, suggesting that MTs mediate FA disassembly (Bershadsky et al., 1996). Several mechanisms were proposed to explain how MT depolymerisation mediates FA assembly (Enomoto, 1996; Krylyshkina et al., 2002). Rho-stimulated myosin activity is one of the essential components in mediating cell contractility, which exerts force to drive FA formation (Chrzanowska-Wodnicka and Burridge, 1996). Inhibition of cell contractility by blebbistatin abolished the nocodazole-induced increase in FA assembly, suggesting that MT disruption enhances the force exerted by the actin cytoskeleton on FAs (Bershadsky et al., 1996). Hence, the state of MT assembly might regulate the tension at FAs. GEF-H1 is a MT-bound guanine nucleotide exchange factor for RhoA, and its activity is increased upon its release from MTs (Krendel et al., 2002; Matsuzawa et al., 2004; Ren et al., 1998). Demonstration that GEF-H1 mediates RhoA activation after nocodazole treatment provides a possible mechanism behind the regulation of cell contractility by the state of MT assembly (Chang et al., 2008). Kinesin is another player implicated in adhesion regulation by MTs. Inhibition of kinesin prevents adhesion disassembly despite normal MT targeting to adhesions, suggesting that MTs regulate adhesion disassembly via a kinesin-mediated cargo transport to adhesions (Krylyshkina et al., 2002). MT depolymerisation disrupts this kinesin-mediated cargo transport, thus preventing adhesion disassembly and facilitating adhesion enlargement. By contrast, we observe here that the ER, a kinesin cargo, promotes FA assembly even though bare MTs (without ER) facilitate FA disassembly. The ER seems to antagonize the role of MTs in FA dynamics (Fig. 8, S3). FA plaque sizes at the cell periphery for ER+, MT+ and ER–, MT– cells are similar, suggesting a basal steady-state level of plaque growth dynamics. For ER–, MT+ cells, plaque sizes are reduced, and for ER+, MT– cells, plaques are significantly enlarged, relative to the basal level. Therefore, MTs facilitate FA disassembly whereas the ER promotes FA assembly. This raises a number of further questions, namely how is the basal steady-state level of plaque size maintained or regulated when both MTs and ER are contacting FAs, and what is the purpose of the antagonistic regulation of FA dynamics by MTs and ER? These and other questions derived from our observations require further investigation.

Dynamic targeting of the ER to FAs might constitute a novel mechanism in adhesion regulation. Disruption of proper ER extension would result in abnormal localisation of the ER and could affect numerous pathways that are essential for FA formation. The ER, a multi-functional organelle, can act as Ca^{2+} reservoir and as a resource for synthesis and modification of proteins and lipids. The high affinity of the ER lumen for Ca^{2+} allows Ca^{2+} to be transported efficiently through its network compared with the cytosol, as if it were in a tunnel (Petersen and Verkhratsky, 2007). Ca^{2+} levels at adhesion sites can be modulated by the ER through active release or sequestration of Ca^{2+} (Clapham, 2007). Local

sequestering of Ca^{2+} at FAs by the ER might reduce the Ca^{2+} transient that is responsible for focal complex disassembly (Conklin et al., 2005). The ER might also modulate Ca^{2+} levels via Stim1, an ER-bound protein that oligomerises upon ER Ca^{2+} store depletion and translocates to the plasma membrane, where it induces store-operated Ca^{2+} influx via interaction with Orai1 (Peinelt et al., 2006; Zhang et al., 2005).

FA sites are proposed to be sites for local translational control (Chicurel et al., 1998; Toh et al., 2006). Protein synthesis components such as mRNAs and ribosomes are shown to localise to FAs (Adereth et al., 2005; Chicurel et al., 1998). The recruitment of ER, a major protein synthesis machinery, to FAs might be important for localised translation by actively translating the localised mRNAs of transmembrane FA proteins such as integrins (Adereth et al., 2005). In cultured cells, immunofluorescence studies of the protein elongation eEF1B complex, exhibits an ER-like intracellular distribution associated with kinectin (Ong et al., 2006; Sanders et al., 1996). Hence, the role of the eEF1B complex is intimately associated with ER dynamics. The ER might also participate indirectly in the localised translation of cytosolic FA proteins by localising the protein elongation factors to FAs to facilitate cytosolic protein translation. Localised translation is an interesting mechanism that would allow localised expression of adhesion proteins at FA sites where they are needed. Further experiments should dissect the detailed mechanism of how the ER promotes FA protein recruitment and plaque growth in the cellular lamella.

In summary, the observations presented here indicate that ER is localised to FAs through kinectin-mediated ER extension along MTs. ER localisation to FAs has a positive role in FA assembly, with consequent impact on the regulation of cell shape, spreading and migration. Although MTs have a known negative role in FA dynamics, we propose that MTs can also have a positive role when the kinectin–kinesin complex delivers ER to FAs, where the ER exerts a positive effect on FA assembly.

Materials and Methods

Cell culture
HeLa cells were cultured in complete media DMEM (Invitrogen) supplemented with 10% (v/v) Fetal Bovine Serum (FBS; Hyclone) at 37°C in a 5% CO_2 incubator. A stable DsRed2-ER clone was established via transfection of pDsRed2-ER (Clontech) into cells using TransFast transfection reagent (Promega) and selected in the presence of G418 (Invitrogen). KNT[KD] and KNT[VC] are previously established stable cell lines (Santama et al., 2004).

Transient transfection
The cDNA of KNT[+] and KHC[+] domains were individually subcloned into pEGFP-C1 vector (Clontech) (Santama et al., 2004). Full-length mouse cDNA encoding integrin β3 and EGFP were subcloned into pcDNA3 (Ballestrem et al., 2001). Human *KTN1* (hknt-vd4[+]) cloning strategy was based on GenBank accession number Z22551 and subcloned into pEGFP-C1. Empty vectors were used as controls for all experiments. Cells were seeded onto 15 mm coverslips or 35 mm glass-bottom dishes overnight and transfected with their respective plasmids using Lipofectamine 2000 transfection reagent (Invitrogen) as per the manufacturer's instructions. Assays were carried out 24–48 hours after transfection.

Microinjection study
Mouse *Ktn1* cloning strategy was based on GenBank accession number L43326. Mouse *Ktn1* cDNA containing (mknt-vd4[+]) or lacking the vd4 domain (mknt-vd4[−]) were individually constructed by subcloning the respective cDNA into pEGFP-N3 vector (Clontech). GenBank accession number of the C-terminal domains of mknt-vd4[+] and mknt-vd4[−] are AJ517376 and AJ517367, respectively. Owing to their large size, these plasmids were microinjected into cells using Eppendorf Micromanipulator 5171 and Transjector 5246 (Eppendorf) coupled to an Olympus IX70 microscope. After microinjection, the cells were kept at 37°C in a 5% CO_2 incubator for 5 hours. Cells were then fixed with 3.7% paraformaldehyde (PFA) and mounted using DakoCytomation Fluorescent Mounting Medium (Dako) onto glass slides for confocal imaging.

Cell spreading assay
Transfected cells or cells stained with CellTracker Green (Invitrogen) were trypsinised, re-seeded onto 35 mm glass-bottom dishes and placed in a CO_2, humidity and temperature controlled stage incubation chamber (MIU-IBC-I, Olympus) and imaged using an Olympus FluoView1000 confocal microscopy at 5 minute intervals for 12 hours. Cell areas were delineated and projected cell area quantified using ImageJ (National Institutes of Health, USA).

Chemotaxis-induced cell migration assay
5×10^4 cells were resuspended in serum-free DMEM, seeded onto the upper membrane surface of 12 mm polycarbonate Transwell inserts (Millipore) with pore size of 8.0 µm and placed in a 24-well plate. DMEM containing 10% FBS was then added into the wells, contacting the lower membrane surface of the inserts to generate a serum concentration gradient. Cells were allowed to migrate at 37°C in a 5% CO_2 incubator for 3 hours. Cells on the inserts were then fixed with 3.7% PFA. Cells remaining on the upper membrane surface of the insert were removed. Cells on the lower membrane surface of the insert were stained with Trypan Blue solution (Fluka Chemika). Images of the cells on each insert were captured using light microscopy (Olympus IX50) and cell numbers in each image were quantified using ImageJ software. Migration was calculated as the percentage of cells that migrated to the lower membrane surface after 3 hours.

Wound healing cell migration assay
Cells were seeded in 24-well plates and cultured to confluence overnight. The cell monolayer was scratched in the middle with a pipette tip to create a wound. Cells adjacent to the wound migrated into the wound. Images were captured using a light microscope at 0 and 24 hour after wounding. Wound area was measured using ImageJ. Migration was calculated as the percentage of wound area healed after 24 hours.

Immunofluorescence staining
Cells cultured on coverslips were fixed with 3.7% PFA for 10 minutes at 37°C and permeabilised with 0.1% Triton X-100 (Sigma) for 5 minutes at room temperature (RT). Fixed cells were blocked with 1% bovine serum albumin (BSA; Sigma) in PBS for 1 hour at RT before incubation with appropriate primary antibodies: anti-calreticulin (Stressgen), anti-cortactin (Santa Cruz), anti-paxillin or anti-vinculin (Sigma) at 4°C overnight. Cells were then incubated for 1 hour at RT with appropriate secondary antibodies: Alexa-Fluor-405-conjugated anti-mouse IgG, Alexa-Fluor-405-conjugated anti-rabbit IgG or FITC-conjugated anti-mouse IgG (Molecular Probes[®] Invitrogen). Coverslips were then washed with PBS and mounted in DakoCytomation Fluorescent Mounting Medium (Dako) on glass slides. For MT fixation, cells were fixed with 4% PFA and 0.02% glutaraldehyde at RT for 20 minutes and permeabilised with 0.1% Triton X-100 for 5 minutes at RT. MTs were labelled using anti-tubulin monoclonal antibody (Sigma). For nocodazole treatment, cells were treated with 1 µM nocodazole (Sigma) in DMEM containing serum for 2 hours at 37°C in a 5% CO_2 incubator. Control cells were treated with 0.1% DMSO instead of nocodazole.

Confocal microscopy
Fixed cells were imaged using LSM510 Meta (Zeiss) or FluoView1000 (FV1000; Olympus) confocal microscopes. DsRed2-ER visualisation was achieved via a 543 nm HeNe (LASOS) laser for LSM510 Meta and 543 nm HeNe (Melles Griot) laser for FV1000. BP565-615 and BA560 IF filters were used to collect the emitted fluorescence respectively. The GFP-fused protein and FITC-conjugated antibody stained proteins were excited by 488 nm MultiArgon (LASOS) laser for LSM510 Meta and 488 nm MultiArgon (Melles Griot) laser for FV1000. LP505 and BA505-525 filters collected the emitted fluorescence respectively. A 405 nm Diode (Melles Griot) laser was used to provide the excitation for Alexa-Fluor-405-conjugated antibody-stained proteins in the FV1000. Plan-NeoFluar 100×/1.30 oil-immersion objective lens (Zeiss) and PlanAPO 100×/1.45 TIRFM lens (Olympus) were used respectively. Live cells were imaged using FV1000 confocal microscope equipped with a stage incubation chamber. The objective used was UPlan Apochromat 60×/1.35 oil immersion objective lens (Olympus). For the FRAP experiment, images were acquired on LSM510 Meta equipped with a stage incubation chamber. A pre-bleach image was acquired. Then the region of interest on the cell was bleached with a laser pulse for 20 seconds at 200 mW without scanning. Single section images were then collected at 2-minute intervals.

Image processing
Images with no saturated pixels were obtained using photo multiplier tube (PMT). Imaris software suite (Bitplane AG) was used to generate surface-rendered images. ImageJ software was used to generate a representative threshold mask to provide an accurate cell edge, projected cell area, ER boundary or FAs. Projected cell area and the size and number of the FA plaques were measured quantitatively using the particle analysis function of ImageJ. Quantification of membrane ruffle perimeter was performed using the measure function of ImageJ. The number of paxillin- and vinculin-containing plaques located within 5 µm from the edge of membrane ruffles were normalised against the length of its respective ruffle. Cells were characterised

to have 'normal' ER extension within the cellular lamella if the ER was not retracted greater than 5 μm from the cell edge of membrane ruffles and the cortactin border.

FRAP analysis

A fiducial reference was chosen, relative to which all coordinates were gauged, to ensure the stability of the frame of reference throughout the experimental timeframe. To compensate for the fluctuations in the illumination, a background section was averaged and its intensity used as a standard candle to calibrate the relative image brightness. The rectangular bleach area does not allow for a clean near-exponential recovery curve because of corner effects (Braeckmans et al., 2007). To reduce the effects from the corners of the bleached rectangle, central ROIs were chosen which were subjected to homogeneous diffusion repletion of stained material. The fluorescence recovery measurement was limited to the brightest histogram clusters, hence segmenting out the GFP-labelled plaque. The top 3% of the bright values was discarded to ensure robustness against recording noise. The fluorescence measurement pre-bleach was taken as 100% and immediately post-bleach as 0%. Half-life ($t_{1/2}$) is the time taken for the fluorescence to recover to 50%.

CLIMP-63 siRNA studies

Human *CKAP4* sequence (GenBank accession number NM_006825.2) was used as the template for synthesis of a *CKAP4*-specific siRNA (5′-CCAAAUCCAUCA-ACGACAATT-3 ′), targeting nucleotides 818–836 bp (Sigma). *CKAP4* siRNA was delivered into cells via Lipofectamine 2000. Proteins extracted from cells 48 hours after transfection were separated by SDS-polyacrylamide gel (12.5%) electrophoresis (SDS-PAGE), transferred to PVDF membranes by wet electroblotting and immunoblotted with mouse anti-human CLIMP-63 antibody (Alexis® Biochemicals) and mouse anti-human β-actin antibody (Sigma). The primary antibody binding was processed for ECL detection (Amersham Pharmacia Biotech) with HRP-conjugated anti-mouse IgG (Sigma). β-actin was used as an internal control. Microscopic evaluation of the morphology and organisation of the ER was carried out 48 hours after transfection.

Supplementary material available online at
http://jcs.biologists.org/cgi/content/full/123/22/3901/DC1

References

Abercrombie, M., Heaysman, J. E. and Pegrum, S. M. (1971). The locomotion of fibroblasts in culture. IV. Electron microscopy of the leading lamella. *Exp. Cell Res.* **67**, 359-367.

Adams, J. C. (2001). Cell-matrix contact structures. *Cell. Mol. Life Sci.* **58**, 371-392.

Adereth, Y., Dammai, V., Kose, N., Li, R. and Hsu, T. (2005). RNA-dependent integrin alpha3 protein localization regulated by the Muscleblind-like protein MLP1. *Nat. Cell Biol.* **7**, 1240-1247.

Alexandrova, A. Y., Arnold, K., Schaub, S., Vasiliev, J. M., Meister, J. J., Bershadsky, A. D. and Verkhovsky, A. B. (2008). Comparative dynamics of retrograde actin flow and focal adhesions: formation of nascent adhesions triggers transition from fast to slow flow. *PLoS ONE* **3**, e3234.

Arregui, C. O., Balsamo, J. and Lilien, J. (1998). Impaired integrin-mediated adhesion and signaling in fibroblasts expressing a dominant-negative mutant PTP1B. *J. Cell Biol.* **143**, 861-873.

Balaban, N. Q., Schwarz, U. S., Riveline, D., Goichberg, P., Tzur, G., Sabanay, I., Mahalu, D., Safran, S., Bershadsky, A., Addadi, L. et al. (2001). Force and focal adhesion assembly: a close relationship studied using elastic micropatterned substrates. *Nat. Cell Biol.* **3**, 466-472.

Ballestrem, C., Wehrle-Haller, B., Hinz, B. and Imhof, B. A. (2000). Actin-dependent lamellipodia formation and microtubule-dependent tail retraction control-directed cell migration. *Mol. Biol. Cell* **11**, 2999-3012.

Ballestrem, C., Hinz, B., Imhof, B. A. and Wehrle-Haller, B. (2001). Marching at the front and dragging behind: differential alphaVbeta3-integrin turnover regulates focal adhesion behavior. *J. Cell Biol.* **155**, 1319-1332.

Baumann, O. and Walz, B. (2001). Endoplasmic reticulum of animal cells and its organization into structural and functional domains. *Int. Rev. Cytol.* **205**, 149-214.

Berman, A. E., Kozlova, N. I. and Morozevich, G. E. (2003). Integrins: structure and signaling. *Biochemistry* **68**, 1284-1299.

Bershadsky, A., Chausovsky, A., Becker, E., Lyubimova, A. and Geiger, B. (1996). Involvement of microtubules in the control of adhesion-dependent signal transduction. *Curr. Biol.* **6**, 1279-1289.

Borm, B., Requardt, R. P., Herzog, V. and Kirfel, G. (2005). Membrane ruffles in cell migration: indicators of inefficient lamellipodia adhesion and compartments of actin filament reorganization. *Exp. Cell Res.* **302**, 83-95.

Braeckmans, K., Remaut, K., Vandenbroucke, R. E., Lucas, B., De Smedt, S. C. and Demeester, J. (2007). Line FRAP with the confocal laser scanning microscope for diffusion measurements in small regions of 3-D samples. *Biophys. J.* **92**, 2172-2183.

Chambers, A. F., Groom, A. C. and MacDonald, I. C. (2002). Dissemination and growth of cancer cells in metastatic sites. *Nat. Rev. Cancer* **2**, 563-572.

Chang, Y. C., Nalbant, P., Birkenfeld, J., Chang, Z. F. and Bokoch, G. M. (2008). GEF-H1 couples nocodazole-induced microtubule disassembly to cell contractility via RhoA. *Mol. Biol. Cell* **19**, 2147-2153.

Chhabra, E. S. and Higgs, H. N. (2007). The many faces of actin: matching assembly factors with cellular structures. *Nat. Cell Biol.* **9**, 1110-1121.

Chicurel, M. E., Singer, R. H., Meyer, C. J. and Ingber, D. E. (1998). Integrin binding and mechanical tension induce movement of mRNA and ribosomes to focal adhesions. *Nature* **392**, 730-733.

Choi, C. K., Vicente-Manzanares, M., Zareno, J., Whitmore, L. A., Mogilner, A. and Horwitz, A. R. (2008). Actin and alpha-actinin orchestrate the assembly and maturation of nascent adhesions in a myosin II motor-independent manner. *Nat. Cell Biol.* **10**, 1039-1050.

Chrzanowska-Wodnicka, M. and Burridge, K. (1996). Rho-stimulated contractility drives the formation of stress fibers and focal adhesions. *J. Cell Biol.* **133**, 1403-1415.

Clapham, D. E. (2007). Calcium signaling. *Cell* **131**, 1047-1058.

Conklin, M. W., Lin, M. S. and Spitzer, N. C. (2005). Local calcium transients contribute to disappearance of pFAK, focal complex removal and deadhesion of neuronal growth cones and fibroblasts. *Dev. Biol.* **287**, 201.

Cory, G. O. and Ridley, A. J. (2002). Cell motility: braking WAVEs. *Nature* **418**, 732-733.

Enomoto, T. (1996). Microtubule disruption induces the formation of actin stress fibers and focal adhesions in cultured cells: possible involvement of the rho signal cascade. *Cell Struct. Funct.* **21**, 317-326.

Geiger, B., Spatz, J. P. and Bershadsky, A. D. (2009). Environmental sensing through focal adhesions. *Nat. Rev. Mol. Cell Biol.* **10**, 21-33.

Heath, J. P. and Holifield, B. F. (1991). Cell locomotion: new research tests old ideas on membrane and cytoskeletal flow. *Cell Motil. Cytoskeleton* **18**, 245-257.

Hernandez, M. V., Sala, M. G., Balsamo, J., Lilien, J. and Arregui, C. O. (2006). ER-bound PTP1B is targeted to newly forming cell-matrix adhesions. *J. Cell Sci.* **119**, 1233-1243.

Hinz, B., Alt, W., Johnen, C., Herzog, V. and Kaiser, H. W. (1999). Quantifying lamella dynamics of cultured cells by SACED, a new computer-assisted motion analysis. *Exp. Cell Res.* **251**, 234-243.

Hu, J., Shibata, Y., Voss, C., Shemesh, T., Li, Z., Coughlin, M., Kozlov, M. M., Rapoport, T. A. and Prinz, W. A. (2008). Membrane proteins of the endoplasmic reticulum induce high-curvature tubules. *Science* **319**, 1247-1250.

Humphries, J. D., Wang, P., Streuli, C., Geiger, B., Humphries, M. J. and Ballestrem, C. (2007). Vinculin controls focal adhesion formation by direct interactions with talin and actin. *J. Cell Biol.* **179**, 1043-1057.

Ingram, V. M. (1969). A side view of moving fibroblasts. *Nature* **222**, 641-644.

Kaverina, I., Krylyshkina, O. and Small, J. V. (1999). Microtubule targeting of substrate contacts promotes their relaxation and dissociation. *J. Cell Biol.* **146**, 1033-1044.

Klopfenstein, D. R., Kappeler, F. and Hauri, H. P. (1998). A novel direct interaction of endoplasmic reticulum with microtubules. *EMBO J.* **17**, 6168-6177.

Krendel, M., Zenke, F. T. and Bokoch, G. M. (2002). Nucleotide exchange factor GEF-H1 mediates cross-talk between microtubules and the actin cytoskeleton. *Nat. Cell Biol.* **4**, 294-301.

Krylyshkina, O., Kaverina, I., Kranewitter, W., Steffen, W., Alonso, M. C., Cross, R. A. and Small, J. V. (2002). Modulation of substrate adhesion dynamics via microtubule targeting requires kinesin-1. *J. Cell Biol.* **156**, 349-359.

Kumar, J., Yu, H. and Sheetz, M. P. (1995). Kinectin, an essential anchor for kinesin-driven vesicle motility. *Science* **267**, 1834-1837.

Lai, F. P., Szczodrak, M., Block, J., Faix, J., Breitsprecher, D., Mannherz, H. G., Stradal, T. E., Dunn, G. A., Small, J. V. and Rottner, K. (2008). Arp2/3 complex interactions and actin network turnover in lamellipodia. *EMBO J.* **27**, 982-992.

Lauffenburger, D. A. and Horwitz, A. F. (1996). Cell migration: a physically integrated molecular process. *Cell* **84**, 359-369.

Leung, E., Print, C. G., Parry, D. A., Closey, D. N., Lockhart, P. J., Skinner, S. J., Batchelor, D. C. and Krissansen, G. W. (1996). Cloning of novel kinectin splice variants with alternative C-termini: structure, distribution and evolution of mouse kinectin. *Immunol. Cell Biol.* **74**, 421-433.

Matsuzawa, T., Kuwae, A., Yoshida, S., Sasakawa, C. and Abe, A. (2004). Enteropathogenic *Escherichia coli* activates the RhoA signaling pathway via the stimulation of GEF-H1. *EMBO J.* **23**, 3570-3582.

Ong, L. L., Lim, A. P., Er, C. P., Kuznetsov, S. A. and Yu, H. (2000). Kinectin-kinesin binding domains and their effects on organelle motility. *J. Biol. Chem.* **275**, 32854-32860.

Ong, L.-L., Lin, P.-C., Zhang, X., Chia, S.-M. and Yu, H. (2006). Kinectin-dependent assembly of translation elongation factor-1 complex on endoplasmic reticulum regulates protein synthesis. *J. Biol. Chem.* **281**, 33621-33634.

Peinelt, C., Vig, M., Koomoa, D. L., Beck, A., Nadler, M. J., Koblan-Huberson, M., Lis, A., Fleig, A., Penner, R. and Kinet, J. P. (2006). Amplification of CRAC current by STIM1 and CRACM1 (Orai1). *Nat. Cell Biol.* **8**, 771-773.
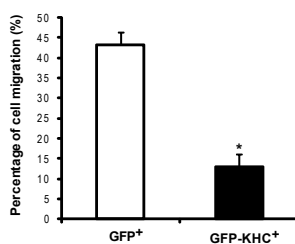
Petersen, O. H. and Verkhratsky, A. (2007). Endoplasmic reticulum calcium tunnels integrate signalling in polarised cells. *Cell Calcium* **42**, 373-378.

Ren, Y., Li, R., Zheng, Y. and Busch, H. (1998). Cloning and characterization of GEF-H1, a microtubule-associated guanine nucleotide exchange factor for Rac and Rho GTPases. *J. Biol. Chem.* **273**, 34954-34960.

Ridley, A. J., Schwartz, M. A., Burridge, K., Firtel, R. A., Ginsberg, M. H., Borisy, G., Parsons, J. T. and Horwitz, A. R. (2003). Cell migration: integrating signals from front to back. *Science* **302**, 1704-1709.

Sanders, J., Brandsma, M., Janssen, G. M., Dijk, J. and Moller, W. (1996). Immunofluorescence studies of human fibroblasts demonstrate the presence of the complex of elongation factor-1 beta gamma delta in the endoplasmic reticulum. *J. Cell Sci.* **109**, 1113-1117.

Santama, N., Er, C. P., Ong, L. L. and Yu, H. (2004). Distribution and functions of kinectin isoforms. *J. Cell Sci.* **117**, 4537-4549.

Taylor, C. W., Prole, D. L. and Rahman, T. (2009). Ca(2+) channels on the move. *Biochemistry* **48**, 12062-12080.

Terasaki, M., Chen, L. B. and Fujiwara, K. (1986). Microtubules and the endoplasmic reticulum are highly interdependent structures. *J. Cell Biol.* **103**, 1557-1568.

Toh, Y.-C., Ng, S., Khong, Y. M., Zhang, X., Zhu, Y., Lin, P.-C., Ten, C.-M., Sun, W. S. and Yu, H. (2006). Cellular responses to a nanofibrous environment. *Nano Today* **1**, 34-43.

Toyoshima, I., Yu, H., Steuer, E. R. and Sheetz, M. P. (1992). Kinectin, a major kinesin-binding protein on ER. *J. Cell Biol.* **118**, 1121-1131.

Tran, H., Pankov, R., Tran, S. D., Hampton, B., Burgess, W. H. and Yamada, K. M. (2002). Integrin clustering induces kinectin accumulation. *J. Cell Sci.* **115**, 2031-2040.

Vicente-Manzanares, M., Choi, C. K. and Horwitz, A. R. (2009). Integrins in cell migration-the actin connection. *J. Cell Sci.* **122**, 199-206.

Voeltz, G. K., Prinz, W. A., Shibata, Y., Rist, J. M. and Rapoport, T. A. (2006). A class of membrane proteins shaping the tubular endoplasmic reticulum. *Cell* **124**, 573-586.

Wang, Q., Herrera Abreu, M. T., Siminovitch, K., Downey, G. P. and McCulloch, C. A. (2006). Phosphorylation of SHP-2 regulates interactions between the endoplasmic reticulum and focal adhesions to restrict interleukin-1-induced Ca2+ signaling. *J. Biol. Chem.* **281**, 31093-31105.

Weed, S. A., Karginov, A. V., Schafer, D. A., Weaver, A. M., Kinley, A. W., Cooper, J. A. and Parsons, J. T. (2000). Cortactin localization to sites of actin assembly in lamellipodia requires interactions with F-actin and the Arp2/3 complex. *J. Cell Biol.* **151**, 29-40.

Welch, M. D. and Mullins, R. D. (2002). Cellular control of actin nucleation. *Annu. Rev. Cell Dev. Biol.* **18**, 247-288.

Wolfenson, H., Lubelski, A., Regev, T., Klafter, J., Henis, Y. I. and Geiger, B. (2009). A role for the juxtamembrane cytoplasm in the molecular dynamics of focal adhesions. *PLoS ONE* **4**, e4304.

Wozniak, M. J., Bola, B., Brownhill, K., Yang, Y. C., Levakova, V. and Allan, V. J. (2009). Role of kinesin-1 and cytoplasmic dynein in endoplasmic reticulum movement in VERO cells. *J. Cell Sci.* **122**, 1979-1989.

Zaidel-Bar, R., Ballestrem, C., Kam, Z. and Geiger, B. (2003). Early molecular events in the assembly of matrix adhesions at the leading edge of migrating cells. *J. Cell Sci.* **116**, 4605-4613.

Zhang, S. L., Yu, Y., Roos, J., Kozak, J. A., Deerinck, T. J., Ellisman, M. H., Stauderman, K. A. and Cahalan, M. D. (2005). STIM1 is a Ca^{2+} sensor that activates CRAC channels and migrates from the Ca2+ store to the plasma membrane. *Nature* **437**, 902-905.

Zhang, X., Jiang, G., Cai, Y., Monkley, S. J., Critchley, D. R. and Sheetz, M. P. (2008). Talin depletion reveals independence of initial cell spreading from integrin activation and traction. *Nat. Cell Biol.* **10**, 1062-1068.
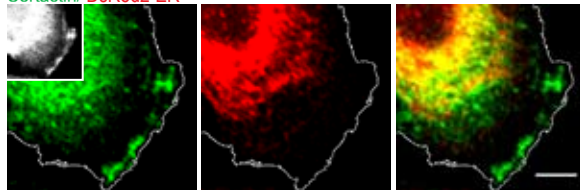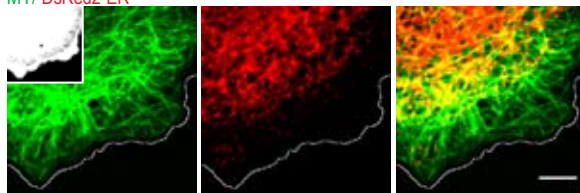
A

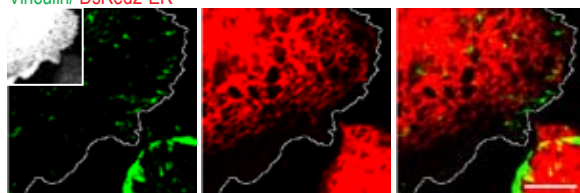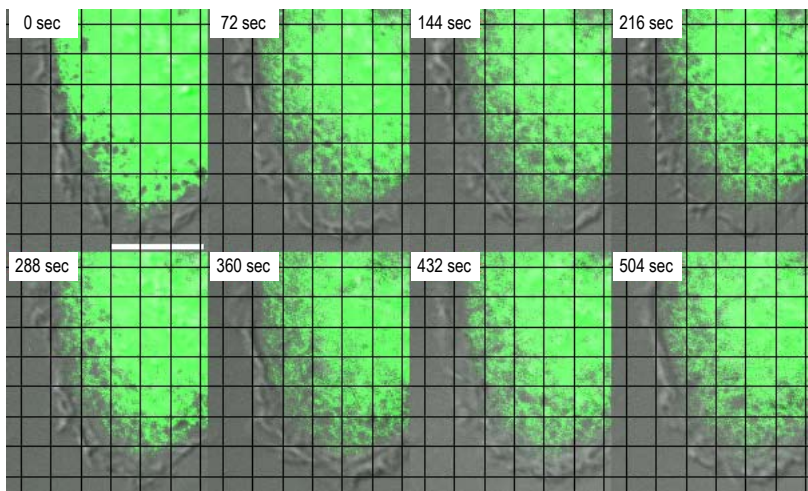Chemotaxis-induced cell migration
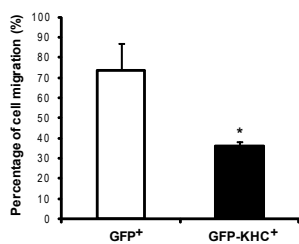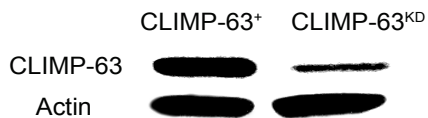
Wound healing cell migration

B

Cortactin/ DsRed2-ER

MT/ DsRed2-ER

Vinculin/ DsRed2-ER

C

0 sec   72 sec   144 sec   216 sec

288 sec   360 sec   432 sec   504 sec

A

CLIMP-63⁺   CLIMP-63^{KD}

CLIMP-63

Actin

B

CLIMP-63⁺

CLIMP-63^{KD}

C

Chemotaxis-induced
cell migration

Wound healing
cell migration

A

B